On the evolution of the viscoelastic properties and their microstructural origin in a filled NBR under coupled thermal and cyclic mechanical loadings

Pierre Garnier, Jean-Benoit Le Cam, Michel Grediac, Marc Dubois, Soraya Ababou-Girard

On the evolution of the viscoelastic properties and their microstructural origin in a filled NBR under coupled thermal and cyclic mechanical loadings

P. Garnier
Innovation Department, PCM Company, Champtocé sur Loire, France

J.-B. Le Cam
Laboratoire de Recherche en Mécanique Appliquée de l'Université de Rennes 1, Université de Rennes 1, Rennes, France

M. Grédiac & M. Dubois
Institut Pascal, Université Blaise Pascal, Clermont Université, Clermont-Ferrand, France

S. Ababou-Girard
Département Matériaux Nanosciences, Université de Rennes 1, Rennes, France

ABSTRACT: This study deals with the effects of coupled thermal and cyclic mechanical loadings on the viscoelastic response of carbon black filled nitrile rubber. For this purpose, cyclic loading tests were performed at different temperatures by means of DMTA. The type and level of the thermomechanical loadings applied were chosen in order to determine the relative contribution of each of the mechanical and thermal loadings (and their coupling) to the viscoelastic response during the cyclic tests. XPS and FTIR analyses were used to track the change in the microstructure corresponding to the evolution in the viscoelastic response. Results show that the storage modulus increases with the number of cycles, due to the crosslink increase, and that temperature amplifies this phenomenon. The main result is that the cyclic mechanical loading significantly amplifies the effect of temperature.

1 INTRODUCTION

Most of the studies dealing with damage in rubbers under mechanical cyclic loading conditions focus on damage, which corresponds to crack initiation and growth until final failure (see for instance Mars and Fatemi (2002)). These purely mechanical studies investigate the effects of uniaxial or multiaxial loading conditions on fatigue damage. Generally, cyclic loading conditions lead to strain level whose amplitude can reach up to several hundreds of percent (Mars and Fatemi 2002, Ostoja-Kuczynski 2005, Andriyana and Verron 2007, Le Cam et al. 2008). However, many industrial applications involve loading conditions and strain levels that are different from the abovementioned ones, in particular compression-compression or relaxing compression with low cyclic strain level at high temperatures. For the nitrile rubbers studied in the present paper, preliminary tests under such loading conditions have shown that damage does not correspond to crack initiation and growth but to a significant change in the microstructure. These changes induce a variation of the initial viscoelastic properties.

The aim of the present paper is first to characterize the change in viscoelastic properties, *i.e.* in the microstructure, in filled nitrile rubber under cyclic compression-compression loading conditions and at various temperatures. Then, the effect of the mechanical loading on the change in the microstructure is investigated in order to define if it influences the response or not. An original cyclic and thermal mechanical test has been carried out for this purpose.

Section 2 deals with the materials and methods used in this study. Results obtained are presented and discussed in Section 3.

2 MATERIAL AND METHODS

2.1 *Material and specimen geometry*

The material tested in this study is a nitrile filled with 35 phr[1] of carbon black, with a small amount of mineral fillers. It was vulcanized with sulphur. The specimens used are bricks of 5 mm heigh with a cross section of $5 \times 5\ mm^2$.

2.2 *Dynamic Mechanical Analysis (DMA)*

The viscoelastic properties of rubber were measured by means of a viscoanalyzer device. The DMA analysis provides the force and displacement signals. The elastic modulus E' and the loss factor $\tan \delta$ are calculated from these data.

2.3 *Loading conditions*

As mentioned above, the tests are aimed at investigating the effect of the thermal and mechanical loadings and their coupling on the microstructure evolution. Two types of tests were performed for this purpose, using different thermal and mechanical loadings. These tests are presented hereafter.

2.3.1 *Coupled thermal and mechanical tests*

The first type of test consisted in applying both a high temperature and a mechanical load at the same time (see Fig. 1-a). The mechanical loading corresponds to a sinusoidal compression at a frequency of 10 Hz.

The tests were performed under prescribed force. Three values of Double Force Amplitude (DFA, defined as the peak-to-peak amplitude) were chosen: 15, 30 and 50 N. For each test, the maximal force value applied was –5 N in order to prevent the specimen to move along the grip during the experiments. Three temperatures were applied: 140, 160 and 180°C. Thus, combined to three mechanical loading levels, nine different tests are defined. During one of the three tests performed at 180°C, another specimen was placed in the temperature-controlled chamber. It serves as a reference specimen, which only underwent the thermal load during the test duration. This leads to ten tests which are described in Table 1. Each test lasted one million cycles.

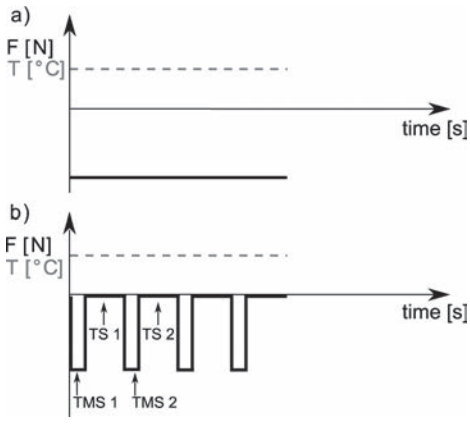

Figure 1. The two different types of thermomechanical loads combining F (solid line) and T (dotted line) used in the study.

[1]Parts per hundred parts of rubber in weight.

2.3.2 *Uncoupled thermal and mechanical tests*

These uncoupled tests are aimed at defining the contribution of the mechanical load on the microstructure evolution under high temperatures levels. The first objective is to observe the viscoelastic properties variations under a constant thermal load. The second objective is to detect possible couplings between temperature and stress. These two objectives are reached by performing a repeated sequence of two loading steps (see Fig. 1):

- during the first step, named the thermal step and denoted TS in the following, only a constant thermal load was applied;
- during the second step, named the thermomechanical step and denoted TMS in the following, the mechanical loading of the first series (15, 30 and 50 N) is applied during 500 cycles.

This sequence is repeated 24 times. Comparing the viscoelastic properties at the end of TMS(i) with those obtained at the beginning of TMS($i+1$) enables one to track their variations during TS(i). Observing the changes in the viscoelastic properties during TMS(i) gives an information about the effect of the coupling between thermal and mechanical loads on the viscoelastic response of

Table 1. Summary of the coupled thermal and mechanical tests.

Name	Temperature [°C]	DFA [N]
T140F15	140	15
T140F30	140	30
T140F50	140	50
T160F15	160	15
T160F30	160	30
T160F50	160	50
T180F15	180	15
T180F30	180	30
T180F50	180	50
T180	180	0

the material. Thanks to each TMS, it was possible to regularly record the mechanical properties during a long heating period. The influence of each TMS on the kinetics of the microstructure change (if any) is assumed to be negligible here because of its very short duration. Nine tests were performed, using the previous combinations of temperature and DFA.

2.4 *Physico-chemical analyses*

Several specimens picked in the series described in section 2.3.2 above were analysed with FTIR spectroscopy. These analyses were performed in order to observe chemical changes in the rubber microstructure after thermal and/or mechanical loads. A virgin specimen was therefore analysed to give the reference spectrum. XPS analyses were also performed on some specimens: T180F50, T180 and a virgin specimen.

3 RESULTS

In this section, results obtained by performing the coupled thermal and mechanical tests are first presented. They are followed by those obtained with the uncoupled mechanical and thermal tests.

3.1 *Coupled thermomechanical loadings*

3.1.1 *Viscoelastic properties evolution*

Figure 2 shows the evolution of E' during the nine tests. For each test, $\Delta E' = E'_{final} - E'_{initial} > 0$, irrespective to the DFA and temperature values. Thus, any combination of temperature and DFA leads to an increase in rigidity. This is an important result since an increase in temperature usually reduces E'. Figure 2 shows the values of $E'_{initial}$ for the six tests performed for a DFA of 30 N and 50 N. These quantities are very close. $E'_{initial}$ is slightly higher for the three tests performed at 15 N. It must be noted that E'_{final} increases when the temperature increases for each DFA. It means that the temperature is one of the causes of the increase in rigidity. Before discussing on the loss factor evolution, these first results must be analyzed in light of the specimen geometry changes during the tests performed at 30 and 50 N. Indeed, there is a flattening which consists in a decrease in height h and in an increase in the cross-section which satisfies the incompressible material hypothesis. As a consequence, the uniaxial Cauchy stress decreases because of the section increase. This phenomenon has a strong impact on the stress and strain levels sustained by the specimens during the tests since these levels are different from the initial ones. Hence considering only the initial stress and strain values and not the current ones could be really misleading.

As a result, this test does not allow us to draw any conclusion concerning the effect of the DFA on the hardening process.

Another point is that no flattening occurs for the lowest DFA (15 N). So the evolution of E' in these cases can only be due to an intrinsic change in the material behaviour. To sum up, an increase in temperature causes an increase in $\Delta E'$ for each DFA. Besides, the effect of the mechanical load on $\Delta E'$ is difficult to evaluate because of the variation in the specimen geometry.

The loss factor tan δ, which is a relevant indicator of the viscous behaviour of the rubber material, also evolves during the tests (see Fig. 3). The main trend for tan δ is a decrease after or not any prior increase. This phenomenon corresponds physically to a decrease in the contribution of the viscosity to the mechanical response. The combined change in E' and tan δ shows that the material evolution consists both in an increase in rigidity and a loss of viscosity at the same time.

This evolution under a high thermal load is expected for a rubber material. It is due to an over-vulcanization, which consists in the recombination of sulphur bonds between macromolecules. Classically, vulcanization of raw blend is obtained by applying a high temperature to the mold. The interesting thing here is that the high temperature is combined to a compressive

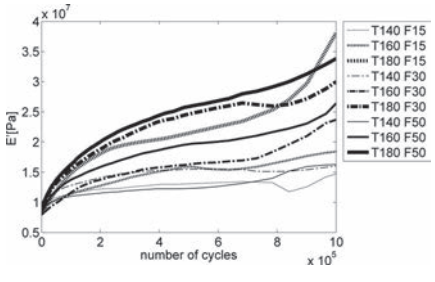

Figure 2. Elastic modulus E' obtained for the nine tests.

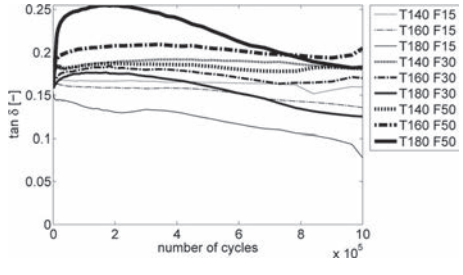

Figure 3. Loss factor tan δ for the nine tests.

loading and the influence on vulcanization is significant.

The evolution of the viscoelastic parameters undoubtedly reflects chemical changes. Suitable chemical analyses were therefore performed to investigate these changes and to evaluate the precise influence of the mechanical loading on vulcanization. Obtained results are presented and discussed in the next section.

3.1.2 *Changes in the rubber microstructure*

FTIR spectra are classically used to observe evolution, creation or disappearance of bonds between elements of interest, *i.e.* changes in the functional groups. Specimens analyzed using the FTIR spectroscopy are described in section 2.4. The corresponding spectra and possible assignments are shown in Figure 4 for the temperature 140°C. Comparison of the FTIR spectra for the single components of the studied materials (not shown here) and the sample after testing does not allow some clear trend to be deduced regarding the position and the relative intensities of the vibration bands. Nevertheless, it can be seen that there is a significant change of the baseline, which decreases in intensity. For each DFA, the spectrum of each specimen after test is beneath that obtained with the virgin specimen. According to Gunasekaran et al. (2007), this shift is due to vulcanization. Indeed, they have studied rubber blends using FTIR spectroscopy. The spectra of vulcanized and reinforced blends are nearly identical and only their rates of absorption differed. The absorption was weaker for vulcanized sample. By analogy, the shift towards low absorption observed in our study could be assigned to the vulcanization. This confirms that every combination of thermomechanical load leads to a certain progress in vulcanization. Besides, the higher the temperature, the lower the intensities of the spectra, thus meaning that the vulcanization rate increases according to the temperature. Moreover, at the same temperature, the higher the DFA, the lower the intensity of the baseline (except at 140°C). It means that vulcanization rate becomes greater at a higher DFA. It was not possible to guess this influence by observing the E' curves of the first series (see Fig. 4), but the changes in specimen geometry may have disturbed the results for the tests at 180°C.

After the coupled thermomechanical tests, uncoupled tests were performed to try to decouple effects of thermal and the mechanical loads.

3.2 *Monitored uncoupled tests*

The variations of E' during the nine tests can be observed on Figure 5. The short TMS was performed to record E' regularly during the thermal load, so that it was possible to track the kinetics of the variations of the viscoelastic parameters during the TMSs. It also gives access to the value of the viscoelastic parameters at the beginning and the end of each TS. During any TS, a quasi-null load was applied (0.1 N) because the viscoanalyser

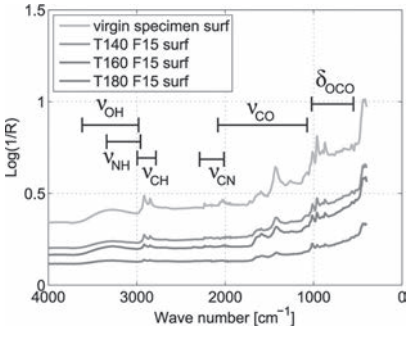

Figure 4. FTIR spectra of the surface of a virgin specimen and specimens after test performed at 15 N at 140, 160 and 180°C.

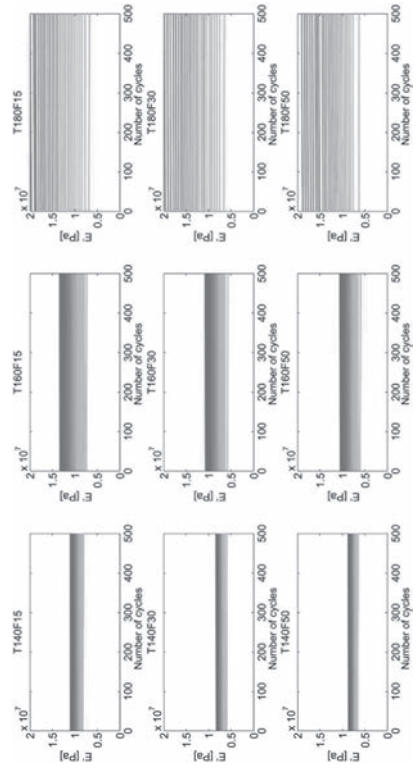

Figure 5. Elastic modulus E' during the 25 thermomechanical steps for the nine sets of thermomechanical parameters.

can not work with a rigorously null load. During each test, the specimen was subjected to a total of 1.25 10^4 cycles (25 TMS of 500 cycles), which is very low compared to the 10^6 cycles applied during the preceding tests. E' is recorded during each TMS (see Fig. 5). Thus, the diagram representing E' during one test contains 25 curves corresponding to the 25 TMSs. The whole campaign is summed up in the 3×3 matrix shown in Figure 5, where in each diagram, the cyan curve corresponds to E' during the first TMS, and the violet one to E' during the last TMS.

The DFA increases along the columns and the temperature along the lines. The sets of curves must be analysed by examining, the width of each group of curves ($\Delta E'$); the height of each group of curves (E'_{init}); the relative position of each successive curve and the monotony of each curve. Some differences clearly appear between these nine results:

- for a given DFA, E'_{final} increases when the temperature increases while E'_{init} remains roughly the same. Hence $\Delta E'$ increases;
- for a given temperature, E'_{init} slightly decreases when the DFA increases and E'_{final} decreases, thus $\Delta E'$ decreases;
- however, the influence of an increase in DFA at 180°C is very low compared to its influence at both 140°C and 160°C.

In conclusion, it can be said that an increase in temperature contributes to the relative increase $\Delta E'$ only, whereas an increase in DFA diminishes both $\Delta E'$ and E'_{init}. The variations of each curve during each TMS also give some very interesting informations about the hardening kinetics. More specifically, the E' variation rate during each TS and TMS ($V_{E'}^{TS}$ and $V_{E'}^{TMS}$) can be calculated as follows:

$$V_{E'}^{TS}(n) = \frac{E_n^{init} - E_n^{final}}{\Delta t_{TS}},\ n = 2,4,6,\ ...,\ 24 \qquad (1)$$

$$V_{E'}^{TMS}(n) = \frac{E_n^{final} - E_n^{init}}{\Delta t_{TMS}},\ n = 1,3,5\ ...,\ 25 \qquad (2)$$

The obtained results are given in Figure 6. The following comments can be drawn for these results during TMS:

- for each test, during the first TMS(s) (between one and three), E' decreases (see the points with a negative coordinate on the curve with the round markers). This phenomenon is probably due to a "demullinization" followed by a general stress softening;
- for a given force, $V_{E'}^{TMS}$ increases when the temperature increases;

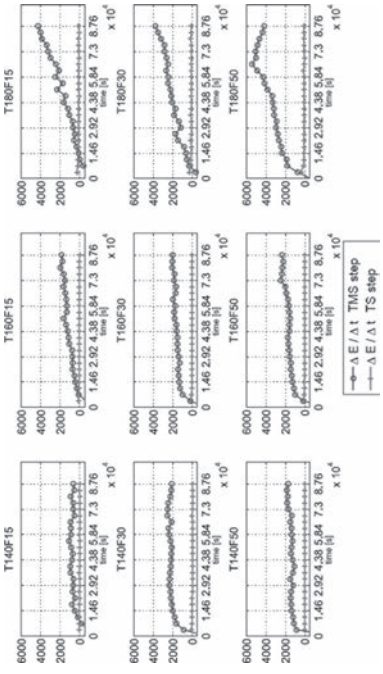

Figure 6. Evolution of the variation rate of E' during each TS and TMS.

- for a given temperature, $V_{E'}^{TMS}$ increases when the DFA increases. This is the first feature showing a positive contribution to the hardening process.

For the first time in the study, it is clearly shown that the mechanical loading has a positive action on stiffening.

3.3 *Chemical bounds investigation*

In the previous section, mechanical tests are analysed to investigate the material response during cyclic loading at several temperatures. It is however not sufficient, using mechanics only, to find the actual causes of the mechanical responses observed during the different types of tests. The idea here is to collect some relevant information about the chemical evolution in order to establish the link with the features of the mechanical response. FTIR spectroscopy and XPS described in Section 2 were used for this purpose.

3.3.1 *X-ray photoelectron spectroscopy*

The analysis is carried out for three different specimens presented in Section 2.4. The piece of material to be analyzed with XPS is extracted from the inside of the specimens after testing. This avoids the need to examine the chemical modifications which might

occur only at the specimen surface during the test. Thus, examining the material located in the inside of the specimen allows us to characterize the changes in microstructure of the bulk material. Figure 7 presents high resolution XPS spectra obtained for each specimen. Curve fitting was used to determine the change in chemical environment of the carbon atoms. These figures present the C_{1s} core levels from the spectra of the virgin, T180 and T180F50 specimens. The C_{1s} core level of the virgin filled nitrile can be fitted by two components. The major one corresponding to the C–C/C–H bonds (284.9 eV) (Zhang 2004) and the lower one, which appears as a shoulder at higher binding energies corresponds to oxidized species (C–O–C/C–OH bonds, 286.3 eV). The C=C bond was included in the C–C component as the gap between these binding energies is only 0.3 eV (Dilsiz and Wightman 2000). From a qualitative point of view, the curve shape and fit do not clearly change between the virgin and heated specimens. This is not really surprising since nitrile rubbers are particularly used for their ability to sustain high temperature without significant changes in their microstructure. Nevertheless, it can be seen in Figure 7-d, which corresponds to specimen T180F50, that the curve obtained significantly differs from the previous ones. This shows that coupling exists between chemical and mechanical effects in the microstructure changes. Indeed, in Figure 7-c we can see a strong reduction of the component at 286.3 eV (C–O bonds) and the appearance of a new component at 288.9 eV that we attribute to O–C=O bonds.

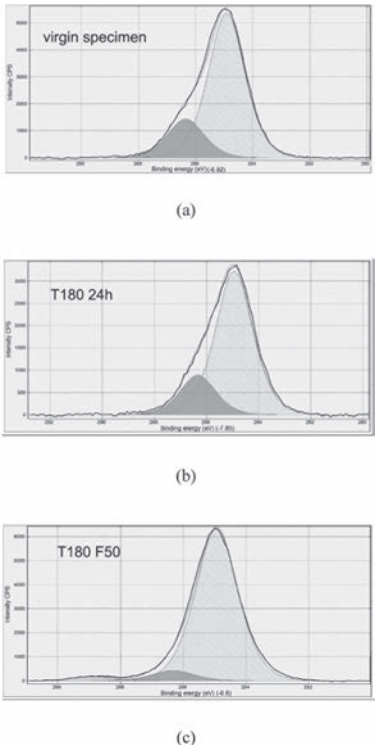

Figure 7. C_{1s} core level peak of the virgin specimen (a), the T180F50 specimen (b), the heated specimen (c).

4 CONCLUSIONS

Two series of cyclic tests have been performed on filled nitrile rubber in order to discriminate the effect of the mechanical loading on the change in the microstructure of filled nitrile rubber under high temperature, typically from 140 to 180 degree Celsius. This change in the microstructure induces an increase in the storage modulus and a decrease in the loss factor. Such evolution appears at high temperature, whatever the mechanical cyclic load (DFA) applied. However, DFA was found to modify the kinetic of change in the microstructure. Indeed, FTIR spectroscopy and XPS analyses have shown that mechanical loading induces changes which or not observed if only a thermal load is applied. Consequently, this study shows that the effects of mechanical loading on filled nitrile rubber tested at high temperatures is significant and cannot be overlooked.

REFERENCES

Andriyana, A. & Verron, E. (2007). Prediction of fatigue life improvement in natural rubber using configurational stress. *International Journal of Solids and Structures 44*, 2079–2092.

Dilsiz, N. & Wightman, J. (2000). Effect of acid-base properties of unsized and sized carbon fibers on fiber/epoxy matrix adhesion. *Colloids and Surfaces A: Physicochemical and Engineering Aspects 164*(2–3), 325–336.

Gunasekaran, S., Natarajan, R. & Kala, A. (2007). FTIR spectra and mechanical strength analysis of some selected rubber derivatives. *Spectrochimica Acta Part A: Molecular and Biomolecular Spectroscopy 68*(2), 323–330.

Le Cam, J.-B., Verron, E. & Huneau, B. (2008). Description of fatigue damage in carbon black filled natural rubber. *Fatigue and Fracture of Engineering Materials & Structures 31*, 1031–1038.

Mars, W.V. & Fatemi, A. (2002). A literature survey on fatigue analysis approaches for rubber. *Int. J. Fatigue 24*, 949–961.

Ostoja-Kuczynski, E. (2005). Comportement en fatigue des élastomères: application aux structures antivibratoires pour l'automobile. Thèse de doctorat, École Centrale de Nantes.

Zhang, S. (2004). In Tribology of Elastomers, Volume 47 of Tri-bology and Interface Engineering Series, pp. 259–265. El-sevier.